REFERENCES AND NOTES

1. D. Schwartz and C. R. Cantor, *Cell* **37**, 67 (1984).
2. L. H. T. Van der Ploeg *et al.*, *ibid.*, p. 77.
3. T. W. Spithill and N. Samaras, *Nucleic Acid Res.* **13**, 4155 (1985).
4. T. W. Spithill and N. Samaras, *UCLA Symp. Mol. Cell. Biol.*, in press.
5. L. H. T. Van der Ploeg and A. W. C. Cornelissen, *Philos. Trans. R. Soc. London B* **307**, 13 (1984); L. H. T. Van der Ploeg *et al.*, *Cell* **39**, 213 (1984); L. H. T. Van der Ploeg, A. W. C. A. Cornelissen, J. D. Barry, P. Borst, *EMBO J.* **13**, 3109 (1984).
6. L. H. T. Van der Ploeg *et al.*, *Science* **229**, 658 (1985).
7. D. J. Kemp *et al.*, *Nature (London)* **315**, 347 (1985).
8. W. C. Gibson, *Parasitology Today*, in press.
9. P. K. Shaw *et al.*, *Am. J. Trop. Med. Hyg.* **25**, 788 (1976); T. L. Gustafson *et al.*, *ibid.* **34**, 58 (1985).
10. Anonymous, *WHO Tech. Rep. Ser. 701* (1984); C. C. Cuba *et al.*, *Trans. R. Soc. Trop. Med. Hyg.* **78**, 708 (1984); N. G. Saravia *et al.*, *Am. J. Trop. Med. Hyg.* **34**, 714 (1985).
11. B. C. Walton and L. Valverde, *Ann. Trop. Med. Parasitol.* **73**, 23 (1979); C. L. Greenblatt, in *New Developments with Human and Veterinary Vaccines*, A. Mizraki *et al.*, Eds. (Liss, New York, 1980), pp. 259–285.
12. The marker strains (abbreviations for figure legends), year of isolation, and geographic origin were: *L. major* WR300 (WR), also held as MHOM/SN/00/DK-106, year unreported; Senegal [described in M. Strobel, B. Ndiaye, C. Renaud-Steens, J. P. Dedet, J. P. Marchand, *Med. Mal. Infect.* **8**, 98 (1978)]; *L. major* D-1 (D1), 1984, from a dog in Egypt (a generous gift of Dr. T. A. Morsy, Ain Shams University, Cairo); *L. donovani chagasi* JBV (Ldc-J), 1984, Maranhaõ, Brazil; *L. donovani chagasi* HBI (Ldc-H), 1984, Bangu, Rio de Janeiro, Brazil; *L. mexicana amazonensis* IOC (Lma-I), 1984, Bahia, Brazil (all three strains were generous gifts of Dr. M. C. de A. Marzochi, Instituto Oswaldo Cruz, Rio de Janeiro); *L. mexicana amazonensis* Josepha (Lma-J), 1975, Brazil [P. D. Marsden, C. C. Cuba, A. C. Barreto, R. N. Sampaio, R. A. A. Rocha, *Trans. R. Soc. Trop. Med. Hyg.* **73**, 391 (1979)]; *L. mexicana mexicana* 1VLM (Lmm), also called WR183, 1958, Panama [M. de V. Coelho and E. Coutinho-Abath, *Rev. Inst. Med. Trop. Sao Paulo* **77**, 136 (1965)]; *L. braziliensis guyanensis* MHOM/SR/80/CUMC-1 (Lbg), 1980, Surinam; *L. braziliensis panamensis* ATCC30879 (Lbp), also held as WR209 and LV641, 1974, Panama [B. E. Beacham, R. Romito, H. D. Kay, *Am. J. Trop. Med. Hyg.* **31**, 252 (1982)]; *L. braziliensis braziliensis* MHOM/PE/83/CUMC-2 (Lbb), 1980, Peru. All strains except D-1 were isolated from humans. We confirmed the nominal identity of each marker strain by typing its isoenzymes of mannose phosphate isomerase (MPI), glyceraldehyde phosphate dehydrogenase (GAPDH1), phosphogluconate dehydrogenase (6PGDH), glucose phosphate isomerase (GPI), and acid phosphatase (ACP). Cultivation of promastigotes [S. H. Giannini, *Trans. R. Soc. Trop. Med. Hyg.* **79**, 458 (1985)] and isoenzyme analysis [R. D. Kreutzer, M. E. Semko, L. D. Hendricks, N. Wright, *Am. J. Trop. Med. Hyg.* **29**, 199 (1980)] have been described.
13. L. H. T. Van der Ploeg, S. H. Giannini, C. R. Cantor, *Science* **228**, 1443 (1985).
14. The α,β-tubulin probe [L. S. Thomashow *et al.*, *Cell* **32**, 35 (1983)], the ribosomal probe Pr8, and the Hsp-70 probe (1.8-kb Hind III 5′ coding region of one of the Hsp-70 genes) (L. H. T. Van der Ploeg *et al.*, unpublished) were all derived from *T. brucei*, like *Leishmania* species a member of the family Trypanosomatidae. Posthybridizational washes were done with 3× SSC (standard saline citrate) at 65°C. All of the genes for which these heterologous probes were used are highly conserved, and the three probes hybridized with leishmanial sequences under the low stringency conditions used. We cannot exclude that there might exist additional divergent copies that were not detected. This possibility does not obscure our analysis of the highly conserved sequences that we did detect.
15. We are grateful to Joan E. Decker-Jackson, Walter Reed Army Institute of Research, for performing the radiorespirometric identification. The patient isolate from Brazil (PtB) had the low profiles of substrate utilization characteristic of *L. braziliensis*. Further details of the technique are in M. L. Chance and B. C. Walton, Ed., *Biochemical Characterization of Leishmania* (UNDP/World Bank/WHO Special Programme for Research and Training in Tropical Diseases, Geneva, 1982).
16. We thank Dianne McMahon-Pratt, Yale University, for the monoclonal antibody typing of the patient isolates. Details of the method are in D. McMahon-Pratt, E. Bennett, J. R. David, *J. Immunol.* **129**, 926 (1982).
17. R. Lainson and J. J. Shaw, in A. M. Fallis, Ed., *Ecology and Physiology of Parasites* (Univ. of Toronto Press, Toronto, 1971), pp. 21–56.
18. C. L. Smith *et al.*, in *Genetic Engineering*, J. K. Setlow and A. Hollaender, Eds. (Plenum, New York), vol. 8, in press; G. F. Carle and M. V. Olson, *Nucleic Acids Res.* **12**, 5647 (1984); A. Bernards *et al.*, *Gene*, in press.

19. We thank S. Azon, W.-M. Ho, and R. Polvere for technical assistance, Dr. C. L. Smith for a gift of lambda size standards, and Dr. N. Agabian for a gift of tubulin clones. Supported in part by a grant from the John D. and Catherine T. MacArthur Foundation and by PHS grants AI-18937, AI-21784, and AI-16282. L.H.T.v.d.P. is a Searle Scholar.

22 January 1986; accepted 3 April 1986

The Mechanism of Binding of a Polynucleotide Chain to Pancreatic Ribonuclease

ALEXANDER MCPHERSON, GARY BRAYER, DUILIO CASCIO, ROGER WILLIAMS

The crystalline complex of pancreatic ribonuclease (RNase) with oligomers of $d(pA)_4$ has been solved by x-ray diffraction methods and refined by standard procedures to a conventional crystallographic R factor of 0.22 at 2.5 angstrom resolution. The asymmetric unit is a complex of one RNase molecule associated with four $d(pA)_4$ oligomers. Although the DNA in this complex is segmented, and therefore shows some discontinuities, it nevertheless traces a continuous path 12 nucleotides in length that passes through the active site cleft of the enzyme and over the surface of the protein. The DNA makes a series of eight to nine electrostatic bonds between its phosphate groups and lysine and arginine residues on the protein, as well as specific chemical interactions at the active site. The path described by the sequence of nucleotides is likely to be that taken by an extended polynucleotide chain when it is bound by the enzyme.

RIBONUCLEASE (RNASE) FROM BOVINE pancreas is among the most thoroughly studied of all protein molecules in terms of structure, chemistry, and enzymatic mechanism (*1–3*). Two functional roles have been ascribed to the protein. Its major function is to cleave RNA at points 3′ to pyrimidine residues to yield fragments having 3′ phosphate termini. A second property of the protein derives from its preferential affinity for, and ability to form complexes with, single-stranded DNA. It is a helix destabilizing or DNA unwinding protein (*4, 5*).

The structure of the protein's active site in the immediate vicinity of enzymatic catalysis has been well established by x-ray and neutron diffraction (*6, 7*), and by chemical

Department of Biochemistry, University of California, Riverside, CA 92521.

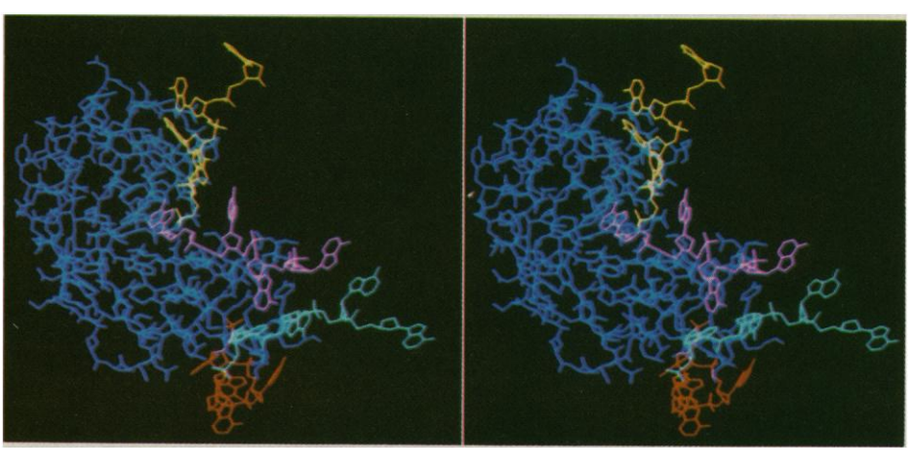

Fig. 1. The structure of the complex formed between bovine RNase A and four tetramers of $d(pA)_4$ as determined by x-ray crystallographic techniques. The four deoxyoligomers I–IV are shown in green, violet, yellow, and red, respectively, and extend in a consistent 3′ to 5′ direction from the top of the figure to the bottom. The conventional crystallographic R factor for the structure at 2.5 Å resolution is 0.22.

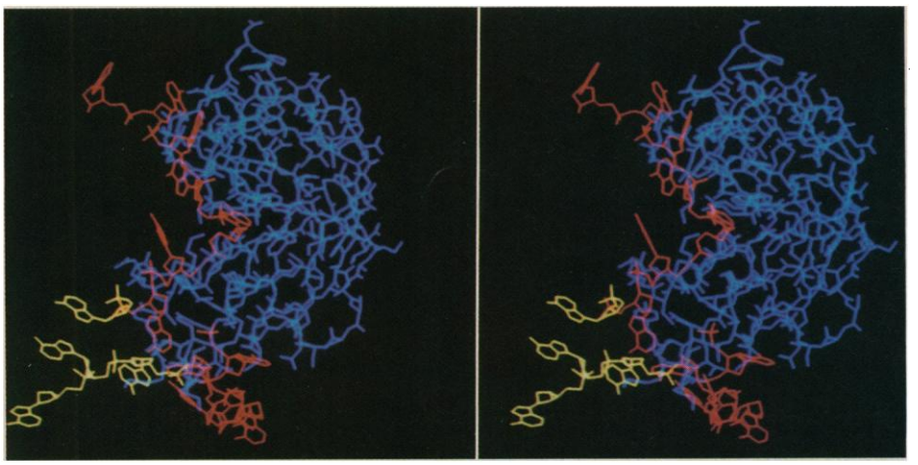

Fig. 2. The complex between bovine RNase and $d(pA)_4$ is shown with those nucleotides (in yellow) from tetramers II and III that are chiefly intermolecular and strongly influenced by lattice contacts. The 12 nucleotides shown in blue are all associated principally with the single red RNase molecule shown in the figure. They can be seen to trace out a nearly continuous path into and through the active site cleft and over the surface of the protein.

modification, spectral, and nuclear magnetic resonance studies (*1, 3*). However, the extended binding interface that mediates association of the protein with long polynucleotide chains has not been well established. This interface, and the constituent interactions, have been shown by competition experiments and other techniques to be the same for both RNA and single-stranded DNA (*8, 9*).

The interaction of polynucleotide and protein, when a stable complex is formed, must involve more of the protein's surface than the restricted cleft shown by difference Fourier experiments to bind dinucleotide substrates (*7, 10*). It must utilize amino acid residues other than His^{12} and His^{119} and Lys^{41}, which have been directly implicated with reasonable certainty in substrate binding and catalysis (*1–3*). Jensen and von Hippel have shown that RNase binds to and protects up to 11 nucleotides along an extended single-stranded nucleic acid chain (*11*). Record *et al.* (*12*), using the same data, subsequently showed by cation titration that at least seven ion pairs, presumably lysine and arginine salt bridges with phosphate groups, are formed when RNase binds to single-stranded DNA. Karpel *et al.* (*13*) have provided further evidence for extensive electrostatic interactions with long substrate analogues devoid of heterocyclic bases. There are numerous studies demonstrating the importance to polynucleotide binding of amino acid side chains distant from the active site (*1–3*) and, by use of electrostatic calculations, Matthew and Richards showed the existence of unusually positive anion binding sites at points well removed from the catalytic center (*14*). The questions that may be asked then are: (i) What path is taken over the surface of RNase by an extended single strand of RNA or DNA when it is bound by the protein? (ii) What chemical interactions between the two macromolecules are involved?

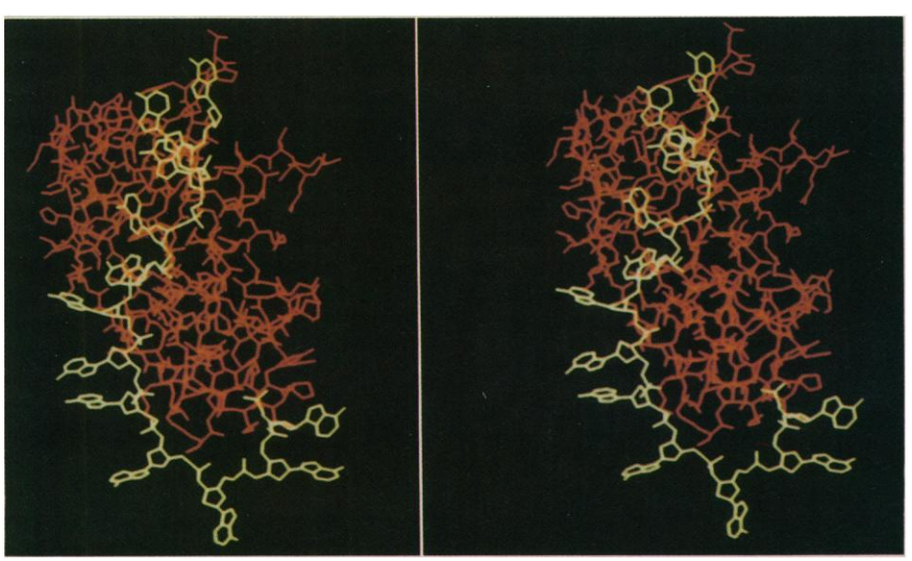

Fig. 3. The 12 blue nucleotides seen in Fig. 2 that are associated with the same RNase molecule have been connected together in a consistent 3′ to 5′ fashion (tetramers I → II → III → IV) to make an extended polynucleotide chain. This virtual strand maintains all of the chemical interactions with the protein that are observed in the crystal structure of the RNase plus $d(pA)_4$ complex (Fig. 1). It has been idealized to some extent in terms of base orientations and backbone conformation.

We succeeded (*15*) in crystallizing complexes of RNase A and RNase B with different deoxyoligonucleotides that included $d(pA)_4$ and $d(pA)_6$. We subsequently obtained other crystalline complexes of RNase with $d(pT)_4$, d(pCTTC), and mixtures of $d(pA)_4$ with $d(pT)_4$. The structures of these complexes have now been solved in this laboratory with x-ray diffraction techniques, and that of the RNase A plus $d(pA)_4$ complex has been refined to an R factor of 0.22 at a resolution of 2.5 Å. The details of the structure solution and refinement have been described (*16, 17*); it is sufficient to say that conventional multiple isomorphous replacement and molecular replacement methods with the known structure of RNase A (*6*) were used, followed by difference Fourier analysis. A somewhat unexpected feature of the results is that the complex of RNase plus $d(pA)_4$ forming the asymmetric unit of the crystals is composed of one protein molecule associated with four independent tetramers of $d(pA)_4$. That is, the stoichiometry of the complex is RNase * $[d(pA)_4]_4$. Similar results were also found for the complexes of RNase plus $d(pA)_6$ and RNase plus $d(pT)_4$.

The disposition of the deoxyoligomers in the complex is not a chance occurrence, but reflects the complementarity of positive charges and nucleotide binding sites on the protein with the negatively charged phosphate groups and bases on an extended nucleic acid chain. The complex of RNase plus $d(pA)_4$ is shown with the four tetramers of nucleic acid in different colors to allow discrimination (Fig. 1).

While a full description of the binding of each of the four oligomers has been presented (*16, 17*), some features are relevant here. Tetramer I runs from its 3′ terminus (Fig. 1, top) into the active site cleft and is positioned with its 5′ terminal phosphate adjacent to His^{12} and Lys^{41} at the active center. The 5′ base is in the conventional "A site" (*2*). Tetramer II has its 3′ terminal nucleotide abutting, but not in fact occupying, the pyrimidine binding site or conventional "P site" (*2*). It passes over the surface of the protein, extends through a solvent region, and terminates with its 5′ phosphate linked

by an electrostatic interaction to another molecule in the crystal lattice. Thus, the first three nucleotides starting from the 3′ end are bound to the molecule shown while the fourth nucleotide at the 5′ end is termed "intermolecular" because it links to a different protein molecule in the crystal lattice.

In tetramer III, only the nucleotide at the 5′ end is bound to the molecule shown (Fig. 1) while the three remaining members of the chain extend through a broad interstitial space in the crystal and terminate with a salt bridge to another protein molecule in the lattice. Thus, fully three nucleotides of tetramer III are intermolecular. Tetramer IV has its 3′ nucleotide adjacent to the 5′ phosphate of tetramer III, curls under the protein, and terminates with its 5′ phosphate in a deep anion trap (*14*) on the backside of the protein.

The arrangement of tetramers (Fig. 1) suggested to us the course a single polynucleotide strand would assume when bound to RNase, even though in these crystals it is composed of oligomeric segments. We noted, furthermore, that the polarity of the $d(pA)_4$ strands was consistently 3′ → 5′ from the top of the figure to the bottom (I → II → III → IV), and that a large number of chemical interactions were used that had been previously implicated by other techniques to be important in nucleic acid binding (*13, 16*).

In Fig. 2, the intermolecular nucleotides are displayed in yellow, and those bound directly to a common RNase molecule are shown in red. The intermolecular interactions are permissible in the crystal only because the asymmetric unit complex contains discontinuous segments that have additional degrees of freedom. We believe that the path delineated in red by the nucleotides bound to this particular RNase molecule are representative of the course traced by a single strand of RNA or DNA when bound to the protein. That is, the $d(pA)_4$ oligomers are a "virtual DNA strand."

If the four yellow nucleotides (Fig. 2) that are involved in the crystalline intermolecular bonds are ignored, then the remaining oligomers and oligomer fragments can be easily linked together in a 3′ to 5′ fashion with no substantial movement of any of the nucleotides, even at the junctures, and with no distortion of either protein or deoxyoligomer conformation. Only the single nucleotide of tetramer III requires any significant rearrangement, and this involves only rotations. The result of this connecting process (Fig. 3) is a continuous single chain of nucleotides, a "virtual strand" extending from the 3′ hydroxyl at the top to the 5′ phosphate at the bottom. In Fig. 3 we have adjusted the bases and the conformation of the ribose-phosphate backbone to some extent to bring the model into a more ideal conformation, but nevertheless it still closely resembles the series of deoxyoligomers that were actually observed in the crystal (Fig. 2) and it preserves all of those interactions responsible for binding.

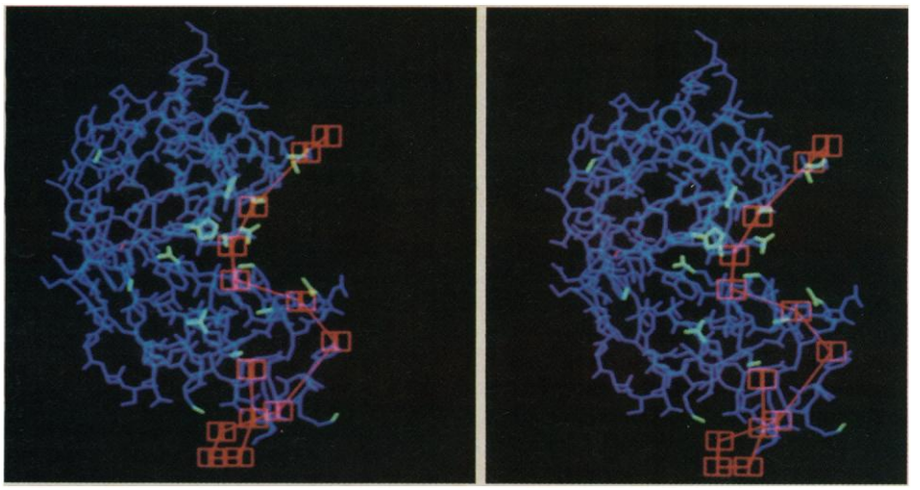

Fig. 4. This schematic drawing of the model complex between RNase plus $d(pA)_4$ shows the pattern of eight to nine electrostatic interactions that bind the polynucleotide to the surface of the protein. These include salt bridges between phosphate groups and Lys^{7}, Lys^{41}, Lys^{66}, Lys^{91}, Lys^{98}, Lys^{31}, and Arg^{85}, Arg^{33}, and Arg^{39}. The only close interactions involving the bases of the nucleic acid with the protein occur in the active site cleft.

A schematic drawing (Fig. 4) of the path taken by the virtual strand of DNA in the model of Fig. 3 shows the protein–nucleic acid interactions observed in the crystal structure that would, by inference, be operative in the protein–nucleic acid complex. Beginning at the 3′ end of the DNA chain and proceeding toward the 5′ terminus, we encounter salt bridges between phosphate groups and Lys^{7}, Lys^{41}, and Lys^{66}, then Arg^{85} and Arg^{39}, then by Lys^{91} and Lys^{98}, then Arg^{33}, and finally Lys^{31}. The only important interactions involving the bases of the DNA occur in the active site at the "P" and "A" sites, and possibly one base removed from the "A" site in the 3′ direction. Other base protein interactions may exist but they are not apparent at this point.

The complex between protein and nucleic acid is principally an extended multisite cation-anion interaction. The base and ribose moieties play only a minor role in binding but, clearly, a major role in determining specificity. This was predicted by Jensen and von Hippel on the basis of their physical chemical data (*11*), and it is entirely consistent as well with the results of Karpel *et al.* (*13*).

The complex contains eight to nine electrostatic "ion pairs." This is very close to the number predicted by Record *et al.* based on cation titrations (*12*). Furthermore, many of the lysine and arginine residues involved in binding were predicted by other investigators (*1–3*). The protein in this complex engages a total of 12 nucleotides, which corresponds to the protection size determined by Jensen and von Hippel (*11*). The virtual strand passes directly through the

Fig. 5. The amino groups of all lysines, the guanidinium groups of arginines, and His^{12} and His^{119} have been highlighted in yellow. The path of the polynucleotide chain is shown in red. The positively charged groups on the protein are disposed as a linear array over the surface of the protein that is closely complementary to the distribution of phosphate groups along an extended nucleic acid chain.

active site cleft in a manner consistent with previous difference Fourier studies using dinucleotides (*7, 10*). The conformation of the polynucleotide chain is smooth, extended, and exhibits no unacceptable turns or bends.

Finally, we would like to call attention to the fact that the 5′ terminus of the polynucleotide strand is firmly bound on the side of the protein opposite the active site, which is nearly 30 Å away from the catalytic center. It is here, as Matthew and Richards showed (*14*), that there is a cluster of lysine and arginine residues precisely where the 5′ terminal phosphate is found. This cluster of Lys^{31}, Lys^{37}, Lys^{91}, and Arg^{33} forms a strong local positive charge distribution that they predicted would serve as a strong anion binding site.

Figure 5 is the RNase molecule with the single DNA strand shown in red, but with lysine amino groups and guanidinium groups of arginines highlighted in yellow along with His^{12} and His^{119}. Apparent in this figure is the linear array of positively charged groups displayed by the protein on its surface and the complementarity between this linear array and the course of the polynucleotide chain. Indeed, we believe that a major consequence of the folding of the polypeptide chain is the presentation of a linear sequence of positive charges in three-dimensional space that traces the path of a polynucleotide chain and serves to lead it through the active site of the enzyme without distortion and in a manner consistent with its chemical and conformational preferences.

REFERENCES AND NOTES

1. C. B. Anfinsen and F. H. White, Jr., in *The Enzymes*, P. D. Boyer, Ed. (Academic Press, New York, ed. 2, 1961), vol. 5.
2. F. M. Richards and H. Wyckoff, in *The Enzymes*, P. D. Boyer, Ed. (Academic Press, New York, ed. 3, 1971), vol. 4.
3. P. Blackburn and S. Moore, in *The Enzymes*, P. D. Boyer, Ed. (Academic Press, New York, ed. 3, 1982), vol. 15.
4. G. Felsenfeld, G. Sandeen, P. H. von Hippel, *Proc. Natl. Acad. Sci. U.S.A.* **50**, 644 (1963).
5. P. H. von Hippel, D. E. Jensen, R. C. Kelly, J. D. McGhee, in *Nucleic Acid-Protein Recognition*, H. J. Vogel, Ed. (Academic Press, New York, 1977).
6. A. Wlodawer and L. Sjolin, *Biochemistry* **22**, 2720 (1983).
7. A. Wlodawer, in *Biological Macromolecules and Assemblies*, F. A. Jurnak and A. McPherson, Eds. (Wiley, New York, 1984), vol. 2, pp. 393–440.
8. F. G. Walz, *Biochemistry* **10**, 2156 (1971).
9. H. Sekine, E. Nakano, K. Sakaguchi, *Biochim. Biophys. Acta* **174**, 202 (1969).
10. H. W. Wyckoff, W. Carlson, S. Wodak, in *Nucleic Acid-Protein Recognition*, H. J. Vogel, Ed. (Academic Press, New York, 1977), pp. 569–580.
11. D. E. Jensen and P. H. von Hippel, *J. Biol. Chem.* **251**, 7198 (1976).
12. M. T. Record, T. M. Lohman, P. de Haseth, *J. Mol. Biol.* **107**, 145 (1976).
13. R. L. Karpel, V. A. Yrttimaa, G. L. Patel, *Biochem. Biophys. Res. Commun.* **100**, 760 (1981).
14. J. B. Matthew and F. M. Richards, *Biochemistry* **21**, 4989 (1982).
15. G. D. Brayer and A. McPherson, *J. Biol. Chem.* **257**, 3359 (1981).
16. A. McPherson, G. D. Brayer, R. Morrison, *Biophysical J.* **49**, 109 (1986).
17. A. McPherson *et al.*, *J. Mol. Biol.*, in press.

18. Supported by grant 21398 from NIH (A.M.). G.D.B. was a recipient of a fellowship from the Canadian Medical Research Council. We thank Ms. Marie Greene and Mr. Gregory DeLozier for production of graphics and Ms. Lindsay Robinson for technical assistance.

9 December 1985; accepted 1 April 1986

Identification and Characterization of the Protein Encoded by the Human N-*myc* Oncogene

DENNIS J. SLAMON, THOMAS C. BOONE, ROBERT C. SEEGER, DUANE E. KEITH, VICKI CHAZIN, HYUN C. LEE, LAWRENCE M. SOUZA

The human N-*myc* gene is related to the c-*myc* proto-oncogene, and has been shown to have transforming potential in vitro. Many studies have reported amplification of N-*myc* in human neuroblastoma and retinoblastoma cell lines. In primary tumors, amplification of the gene was found to correlate directly with behavior of the tumor. Specific restriction fragments of a partial complementary DNA clone of N-*myc* from LA-N-5 human neuroblastoma cells were placed into a bacterial expression vector for the purpose of producing antigens representative of the N-*myc* protein. Rabbits immunized with these antigens produced antisera that recognized a protein of 62–64 kilodaltons in neuroblastoma cells. By several criteria, this protein appears to be part of the same proto-oncogene family as the c-*myc* protein. Moreover, the antisera to fragments of this protein were capable of histochemically identifying malignant cells in clinical specimens.

THE N-*MYC* GENE, WHILE NOT A classic proto-oncogene in that it does not have a homolog carried by an acutely transforming retrovirus, is grouped with the proto-oncogenes because of its homology with c-*myc* (*1, 2*). There is clear evidence for the transforming potential of this gene since N-*myc* can substitute for c-*myc* in the co-transformation assay in which secondary rat embryo cells are transformed into tumorigenic cells (*3*). Thus far, the strongest clinical correlation between alteration of a specific proto-oncogene and human neoplasia has been found in studies of the N-*myc* gene in neuroblastomas. This gene was first identified in human neuroblastoma cell lines where homogeneously staining regions (HSR) on chromosomes (*4*) or double minute (DM) chromosomes (*5*) were frequent. In these cell lines there is a 25- to 700-fold amplification of a gene that is related to, but distinct from, the c-*myc* proto-oncogene (*1, 2*). Amplification and/or increased expression of this gene has been found in untreated primary human neuroblastomas (*6*) and retinoblastomas (*7*). Initial studies of primary neuroblastomas demonstrated that amplification of N-*myc* was correlated with stage of disease; amplification was not found in localized tumors (stages I and II), but was present in 50% of advanced tumors (stages III and IV) (*6*). In a larger study, amplification of the gene in primary neuroblastomas was found to correlate strongly with rapid disease progression and poor clinical prognosis, independent of disease stage at diagnosis (*8*). Thus, amplification of the N-*myc* gene appeared to be more prognostic than clinical staging of the disease.

The strong correlation between N-*myc* gene alterations in primary human tumors and clinical behavior, as well as the transforming potential of the gene in vitro, has led to speculation that it may be involved in the pathogenesis of some human malignancies. To further characterize this gene and its gene product, we undertook experiments to clone and express human N-*myc*. By means of the Okayama-Berg vector (*9*), a complementary DNA library was constructed from the LA-N-5 human neuroblastoma cell line. Approximately 80,000 clones were screened with the pNb-1 probe (*1*), and one clone, N-*myc*1, was obtained. The largest open reading frame in the sequence from N-*myc*1

D. J. Slamon and D. E. Keith, Division of Hematology-Oncology, Department of Medicine, and Jonsson Comprehensive Cancer Center, UCLA School of Medicine, Los Angeles, CA 90024.
T. C. Boone, V. Chazin, L. M. Souza, Amgen, Thousand Oaks, CA 91320.
R. C. Seeger and H. C. Lee, Department of Pediatrics, Jonsson Comprehensive Cancer Center, and Childrens Cancer Study Group, UCLA School of Medicine, Los Angeles, CA 90024.